Truncated versus Extended Microfilms at a Vapor-Liquid Contact Line on a Heated Substrate

Journal:	*Langmuir*
Manuscript ID:	la-2010-02065c.R2
Manuscript Type:	Article
Date Submitted by the Author:	n/a
Complete List of Authors:	Rednikov, Alexey; Université Libre de Bruxelles, TIPs-Fluid Physics, CP 165/67 Colinet, Pierre; Université Libre de Bruxelles, TIPs-Fluid Physics, CP 165/67

Truncated versus Extended Microfilms at a Vapor-Liquid Contact Line on a Heated Substrate

A. Ye. Rednikov* and P. Colinet*

TIPs - Fluid Physics, Université Libre de Bruxelles, CP 165/67, 50 Av. F. D. Roosevelt, B-1050 Brussels, Belgium

E-mail: aredniko@ulb.ac.be; pcolinet@ulb.ac.be

Abstract

The microstructure of a contact line formed by a liquid and its pure vapor on a perfectly-wetted superheated smooth substrate, with the disjoining pressure most often in the form of a positive inverse cubic law (non-polar case), is routinely considered to end up in a microfilm extended over adjacent "dry" parts of the solid surface. Invoking the spreading coefficient as an additional independent parameter within this framework, we argue however that a regime with a truncated microfilm is chosen instead if the spreading coefficient is decreased below a positive (still perfect wetting) critical value dependent upon the superheat, in which case the extended-microfilm thickness is surpassed by that of the "pancake" introduced by de Gennes and coworkers. Conversely, for a given positive spreading coefficient, there is a critical superheat above which the microfilm gets truncated, whereas for a negative one (partial wetting) the truncated regime should be preferred at any superheat. A parametric study of the apparent contact angle (a nonlinear eigenvalue of the steady microstructure problem) versus the spreading coefficient is carried out. When the latter is negative, Young's law is asymptotically recovered. Microfilm fronts are shown to be advancing or receding in accordance with the selected

*To whom correspondence should be addressed

regime. A slightly more general class of disjoining pressures is also touched upon. The analysis is based in part upon thermodynamic considerations, and in part upon a standard one-sided model of an evaporating liquid layer in the lubrication approximation.

I. Introduction

The advent of the theory of the thin-film forces,[1] the salient manifestation of which is in the form of the disjoining pressure, marks a crucial point for our understanding of the contact line (micro)physics.[2] In the case of a perfectly wetting liquid overlaid with its pure vapor on a superheated smooth substrate, it is the thin-film forces that are responsible for a microfilm appearing, in accordance with Potash and Wayner[3] and subsequent studies (see below), on the solid surface ahead of the contact line and in principle extending all over the surface not occupied by the macroscopic portions of the liquid. From the thermodynamic viewpoint, the microfilm appears as a result of equilibrium with the vapor at the temperature of the substrate, higher than the saturation temperature corresponding to the pressure of the vapor, this temperature difference being referred to as the superheat. Such an equilibrium shift is in essence a version of the Kelvin effect, where the disjoining pressure substitutes the Laplace one in its more familiar version. Thus, as far as the (micro)structure of the contact line is concerned, the macroscopic portion of the liquid ends up in an extended microfilm, so that there is effectively no triple line between the liquid, the vapor and the solid, as one can see in Figure 1 (left), where some of the notations and concepts are explained later on in section II. Moosman and Homsy[4] provided a first consistent analysis of this kind of microstructure. Thereafter, this has been a paradigm widely employed in the studies of both steady[5–7] (contact line at rest) and unsteady[8] situations involving a perfectly wetting liquid in contact with its own vapor on a superheated surface. The mentioned studies deal with the case of non-polar liquids, and so will be the case in the present paper. In particular, this concerns the disjoining pressure in the form of an inverse cubic law.

Since, within such a configuration, the vapor-liquid and the liquid-solid surfaces do not ap-

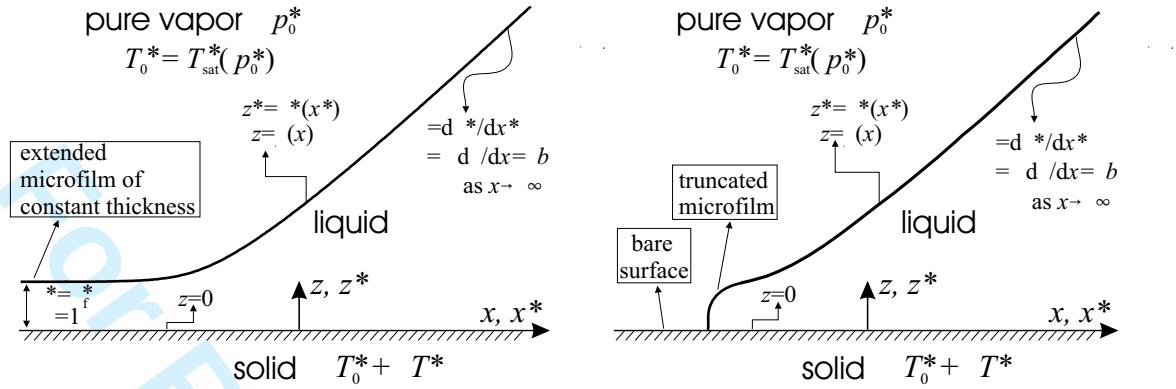

Figure 1: Microstructure of a contact line between a liquid, its pure vapor and a superheated (relative to the saturation temperature at the pressure of the vapor) solid: a sketch. At one end, a constant slope (apparent contact angle) is asymptotically attained in the case of a motionless contact line and a negligible (on the microscale) macroscopic curvature. At the other end, the microstructure terminates in either an extended microfilm (left), or rather a truncated one (right).

proach each other more than at a certain distance (viz. the microfilm thickness), the structure is formally determined just by a relatively high-thickness "tail" of the disjoining pressure isotherm (a positive decreasing function of the thickness at large values of the latter), with no regard for further properties of the vapor-liquid-solid contact such as the spreading coefficient (the difference between the vapor-solid surface tension and the sum of the vapor-liquid and the liquid-solid ones). However, it can be suspected that these properties do matter. For instance, the positiveness of the tail does not necessarily imply a positive spreading coefficient (i.e. perfect wetting), as it does not e.g. when a finest layer of partially wetted material is deposited over the surface of a perfectly wetted solid (as considered by de Gennes et al.,[9] see their figure 4.5b), resulting in a negative spreading coefficient. For such a case, it would be natural to suspect that the contact line regime with an extended microfilm is just metastable and abandoned in favor of a different regime if perturbed sufficiently strongly. If so, one may think it is the positiveness of the spreading coefficient that is a sufficient condition against such metastability (after all, in the mentioned studies, it is typically stated that the analysis is intended just for the case of perfect wetting). In fact, as we show in the present paper, this is not quite so, which can be expected already on the basis of the following heuristic considerations.

Consider a sufficiently small but positive (perfect wetting) value of the spreading coefficient.

With the disjoining pressure tail as we have here, there can exist a "pancake" in the sense put forth by Joanny and de Gennes[10] (see also other works[2,9,11]). It is a puddle of a given macroscopic volume of a non-volatile liquid that no longer spreads on the solid surface. The pancake (of a large volume) has quite a definite thickness depending on the material properties of the system, the spreading coefficient among them. Now turning to the extended microfilm, we know that its thickness decreases with the superheat. Its decrease below the pancake thickness can be suspected as passing through a sort of critical condition, which could well correspond to a transition to another regime (the extended-microfilm regime becoming metastable). And recall that, if this occurs, it is for a positive value of the spreading coefficient, i.e. perfect wetting, which brings us back to the point at the end of the previous paragraph.

An alternative sort of contact line microstructure that can be conjectured in case the extended microfilm is metastable is a structure with a *truncated* microfilm (cf. Figure 1), such that the remainder of the solid surface is just bare (even though Gibbs adsorption on it can actually never be excluded). It is this sort of structure that is of main interest in the present paper.

Thus, to put it differently, the present paper is basically concerned with incorporating the spreading coefficient into the model of a vapor-liquid contact line microstructure on a superheated substrate[3–8] and parametrically investigating some of its consequences. Both positive and negative values of the spreading coefficient will be studied, while the disjoining pressure remains positive. The paradigm used here for the most part (the spreading coefficient plus the disjoining pressure tail, in the form of an inverse cubic law in particular) has often been employed by de Gennes and coworkers[2,9–11] in relation to non-volatile liquids. So, from this viewpoint, the present paper just applies it to the volatile case under consideration.

Some of the features of the model employed elsewhere[3–8] and here include the following. The lubrication approximation is used. The film is shaped by the joint action of disjoining pressure, capillarity and evaporation. Gravity is negligible. The local liquid pressure effect on the local saturation temperature is accounted for, the microfilm equilibrium being in fact a particular manifestation of this (Kelvin) effect. At the same time, the effects of pressure variation and heat

conductivity in the vapor are neglected, which goes along with the one-sided approximation of an evaporating liquid layer. Deviations from local phase equilibrium (the evaporation kinetics) are taken into consideration. Possible temperature inhomogeneities in the solid substrate are neglected. Finally, the Marangoni and the vapor-recoil effects are neglected, which is supported by the analysis carried out elsewhere.[7]

Both the microfilm regime (extended or truncated) and the spreading coefficient (for the truncated regime) in principle influence the overall behavior of the liquid film including the macroscopic scales. In the present paper, we study such an influence while focusing on a small vicinity of the contact line, possessing its own intrinsic scales (microscales). On the microscale, the macroscopic curvature is negligible. Thus one arrives at a configuration with zero curvature towards the macroscopic portion of the liquid (Figure 1). In the steady case (no displacement of the contact line), the film surface just attains a constant slope (Stephan and Busse[5]). This configuration is referred to as the steady microstructure (of a contact line) and is the one considered in the present paper. The constant slope yields the apparent contact angle θ of the microstructure (its intrinsic property), which must be a function of the microfilm regime and of the spreading coefficient in the truncated regime (cf. the above mentioned influence) and is studied as such here. We note that θ must be finite even for perfect-wetting systems and motionless contact lines due to the presence of a (micro)flow induced by the evaporation process and rendering the situation near the contact line always dynamic. Furthermore, the time and velocity scales associated with this microflow are typically rather fast,[7] which permits to expect that the studied *steady* microstructure will hold quasi-steadily even for moving contact lines up to reasonably large velocities and thus increases the value of such a study.

The remainder of the paper is organized as follows. Section II outlines the film configuration (the contact line microstructure) we aim to study here and introduces some basic notations and definitions. Section III analyzes the relative thermodynamic stability of the microfilm against a bare surface in contact with a pure vapor. It is conjectured that it is when the former state is metastable against the latter that the extended-microfilm regime at the contact line is replaced by a truncated-

microfilm one. The outlook of section III is extended in Appendix A, in particular with additional illustrations pertaining to a slightly more general class of disjoining pressures than a positive inverse cubic law. In section IV, we recall a classical form of the film evolution equation (lubrication approximation, one-sided model) to be relied upon in the present study. In section V, the problem for the steady microstructure of a contact line is mathematically formulated, a possible start of a truncated microfilm is analyzed asymptotically, and one of the parameters in the corresponding coordinate expansion gets associated with the spreading coefficient assuming thermodynamic equilibrium at the front edge (the latter being considered in some more detail in Appendix B). A parametric study of the steady microstructure (and first of all, of the apparent contact angle it determines) versus the spreading coefficient is presented in section VI. Traveling microfilm fronts are considered in section VII, confirming in the framework of the film evolution equation that the front is receding under the conditions when the extended microfilm is found to be metastable according to the thermodynamic considerations of section III, and advancing otherwise. Conclusions are presented in section VIII.

II. Problem outline

A triple line between a one-component volatile liquid, its pure vapor and a flat rigid substrate is considered (see Figure 1). The film thickness is denoted by ξ^*, such that the liquid-vapor interface is given by $z^* = \xi^*(x^*)$, where x^* and z^* are the Cartesian coordinates along and across the film, respectively, $z^* = 0$ corresponding to the solid surface. We work in the planar (two-dimensional Cartesian) geometry, when there is no dependence on the third Cartesian coordinate, orthogonal to the plane of Figure 1. In the steady case (considered for the most part in this paper), we just have $\xi^* = \xi^*(x^*)$, as already indicated above. In the unsteady case, however, ξ^* is also a function of the time t^*: $\xi^* = \xi^*(x^*, t^*)$. Here note that the asterisk is used to distinguish dimensional quantities from their dimensionless versions denoted by the same symbol without asterisk and introduced later on in section IV.

Let p_0^* be the pressure in the vapor phase far away from the contact microregion. Define T_0^* as the saturation temperature corresponding to p_0^*, namely, $T_0^* \equiv T_{sat}^*(p_0^*)$. The substrate is kept at a (slightly) higher temperature, $T_w^* \equiv T_0^* + \Delta T^*$, which is actually a definition of the quantity $\Delta T^* > 0$ referred to as superheat. The standard model proceeds from the premise (cf. section I) that the macroscopic portion of the liquid ends up in the form of a microfilm of constant thickness extending all over the available "dry" part of the solid surface, as in Figure 1 (left). The microfilm is in equilibrium with the vapor at the temperature $T_w^* > T_{sat}^*(p_0^*)$ and the vapor pressure p_0^*, owing its existence to the thin-film forces (the disjoining pressure Π^*). As already noted in section I, for the most part of this paper, we limit our attention to the case $\Pi^*(\xi^*) = A^*/\xi^{*3}$ with $A^* > 0$ (which up to a factor 6π and sometimes up to the sign coincides with the Hamaker constant used elsewhere), even though the arguments developed in the present and following sections do not depend on such a specific choice.

Consider the microfilm equilibrium in more detail. Let $\mu_v^* = \mu_v^*(p^*, T^*)$ and $\mu_l^* = \mu_l^*(p^*, T^*)$ be the vapor and liquid chemical potentials, p^* and T^* being the pressure and the temperature. Hereafter, the subscripts 'v' and 'l' refer to the vapor and the liquid, respectively. By the definition of T_0^*, we have $\mu_v^*(p_0^*, T_0^*) = \mu_l^*(p_0^*, T_0^*)$. Define a pressure quantity Δp^* such that $\mu_v^*(p_0^*, T_0^* + \Delta T^*) = \mu_l^*(p_0^* - \Delta p^*, T_0^* + \Delta T^*)$, so that the equilibrium temperature is shifted by ΔT^* (here to the value $T_w^* = T_0^* + \Delta T^*$) owing to a liquid pressure shift by $(-\Delta p^*)$ relative to the gas pressure (the Kelvin effect). Linearizing the difference between the above two equalities of chemical potentials, one arrives at

$$\Delta p^* = \mathscr{L}^* \rho_l^* \Delta T^* / T_0^* \tag{1}$$

where $\mathscr{L}^*$ is the latent heat of evaporation, and ρ^* denotes the density (i.e. ρ_l^* is that of the liquid). The linearization is legitimate for small values of ΔT^* (which are in practice much smaller than T_0^*) and provided that the liquid density does not change any significantly as the pressure drops by Δp^* (incompressibility). In the classical form of the Kelvin effect, Δp^* results from the Laplace (capillary) pressure. In the (flat) microfilm, however, Δp^* is rather associated with the disjoining

pressure so that the microfilm thickness ξ_f^* is determined by

$$\Delta p^* = \Pi^*(\xi_f^*) \tag{2}$$

This equation is obtained later on in a more systematic way, but for the moment note that in the particular case $\Pi^*(\xi^*) = A^*/\xi^{*3}$ with $A^* > 0$, eqs 1 and 2 yield

$$\xi_f^* = \left(\frac{A^* T_0^*}{\mathscr{L}^* \rho_l^* \Delta T^*} \right)^{1/3} \tag{3}$$

As already mentioned, the goal of the present paper is to study, by invoking the spreading coefficient, possible cases when the extended microfilm is absent, being replaced by a truncated one, and the effects this has on the overall configuration shown in Figure 1. To this purpose, before proceeding in section IV with a hydrodynamic model suitable for the configuration in question, it is reasonable to first consider the thermodynamics of the microfilm on account of the spreading coefficient and its possible metastability versus a bare surface (cf. section I).

III. Microfilm Thermodynamics and the Spreading Coefficient

Following Yeh *et al.*,[12,13] we proceed from the ansatz

$$F^* = -p_l^* V_l^* - p_v^* V_v^* + \gamma_{sl}^* \mathscr{A}_{sl}^* + \gamma_{sv}^* \mathscr{A}_{sv}^* + \gamma^* \mathscr{A}_{lv}^*$$

$$+\mu_l^* n_l^* + \mu_v^* n_v^* + \mu_{sl}^* n_{sl}^* + \mu_{sv}^* n_{sv}^* + \int \mathscr{P}^*(\xi^*)\, d\mathscr{A}_{sl}^* \tag{4}$$

Here F^* is the Helmholtz free energy of a finite vapor-liquid system including the solid surface. Equilibrium is already implied within each individual phase involved. $V_l^* = \int \xi^*\, d\mathscr{A}_{sl}^*$ and V_v^* are the volumes of the liquid and vapor phases, whereas n_l^* and n_v^* are their mole numbers. While p_v^* is the vapor pressure, the quantity p_l^* does not have this meaning in the liquid in the presence of the thin-film forces. It should be just regarded as a scalar constant.[12] The chemical potential

$\mu_l^* = \mu_l^*(p_l^*, T^*)$ is the same function of p_l^* as in the classical limit (in the absence of the thin-film forces). $\mathscr{A}_{sl}^*$, $\mathscr{A}_{sv}^*$ and $\mathscr{A}_{lv}^*$ are the areas of the solid-liquid, solid-vapor and liquid-gas interfaces, respectively, γ_{sl}^*, γ_{sv}^* and γ^* are their surface tensions, whereas n_{sl}^* and n_{sv}^*, and μ_{sl}^* and μ_{sv}^* are the corresponding Gibbs surface excess amounts and chemical potentials (no Gibbs adsorption for the liquid-gas interface,[14] and no respective terms present in eq 4). $\mathscr{P}^*(\xi^*)$ is the free energy (per unit area of the film) due to the thin-film forces (here we discard the possible dependence of $\mathscr{P}^*$ on the derivatives of ξ^* and on other thermodynamic quantities). The integration in eq 4 is performed over the solid-surface area occupied by the liquid (film). This may be the entire available solid surface (then $\mathscr{A}_{sv}^* = 0$ and $n_{sv}^* = 0$), or not (then $\mathscr{A}_{sv}^* > 0$). On the other hand, in the case of a bare solid surface (to be also considered below), when no liquid film is present, we have $\mathscr{A}_{sl}^* = \mathscr{A}_{lv}^* = 0$, $V_l^* = 0$, $n_l^* = 0$, $n_{sl}^* = 0$ and in particular the last (integral) term in eq 4 is equal to zero (cf. also the second paragraph of Appendix A). The total volume and the total number of moles are

$$V^* = V_v^* + V_l^*, \quad n^* = n_v^* + n_l^* + n_{sl}^* + n_{sv}^* \tag{5}$$

Now consider a closed macroscopic system consisting of n^* moles of our substance, submitted to an external pressure p_0^* and a temperature $T_w^* = T_0^* + \Delta T^* > T_0^* = T_{sat}^*(p_0^*)$. As a consequence of the second law of thermodynamics, at a constant temperature, spontaneous processes in the system in question occur in such a way that $\Delta F^* \leq W_{ext}^*$, where the term on the left-hand side is the change of the Helmholtz free energy, while the one on the right-hand-side represents the external work on the system. In our case, $W_{ext}^* = -p_0^* \Delta V^*$. Thus, if

$$Z^* \equiv F^* + p_0^* V^* \tag{6}$$

we have $\Delta Z^* \leq 0$, i.e. the system evolves to minimize Z^*. For each equilibrium configuration of the system, the variation of Z^* at constant (total) mass, temperature and external pressure must vanish, i.e. $\delta Z^* = 0$.

More specifically, assuming that $\mathscr{A}^*$ is the area of the solid surface available for condensation

(whose curvature, if any, is negligibly small in the present context), here we shall be interested in comparing two possible zero-dimensional equilibrium states of the system: the one in which the solid surface is covered with a microfilm of constant thickness, itself in contact with the vapor (hereafter referred to as state 'f'), and the one with a bare solid surface directly in contact with the vapor (hereafter state 'b'). Using eqs 4-6 and using the conventions described following eq 4, one can write

$$Z_f^* = (p_0^* - p_v^*)\,V_v^* + (p_0^* - p_l^*)\,V_l^* + (\gamma_{sl}^* + \gamma^*)\,\mathscr{A}^* + \mu_l^*\,n_l^* + \mu_v^*\,n_v^* + \mu_{sl}^*\,n_{sl}^* + \mathscr{P}^*(\xi^*)\,\mathscr{A}^*$$

$$n^* = n_v^* + n_l^* + n_{sl}^*\,, \quad V_l^* = \mathscr{A}^*\,\xi^*$$

for state 'f', and

$$Z_b^* = (p_0^* - p_v^*)\,V_v^* + \gamma_{sv}^*\,\mathscr{A}^* + \mu_v^*\,n_v^* + \mu_{sv}^*\,n_{sv}^*\,, \quad n^* = n_v^* + n_{sv}^*$$

for state 'b'. In equilibrium, the variations must be equal to zero: $\delta Z_f^* = 0$, $\delta Z_b^* = 0$ (for these two states, the variations must be taken also at a constant area $\mathscr{A}^*$). These conditions will permit determining the unknowns remaining for each state, thus finalizing the calculation of the values Z_f^* and Z_b^* themselves. Comparing Z_f^* with Z_b^*, one will be able to judge upon the relative stability of the two states in question: should $Z_f^* - Z_b^* > 0$, state 'f' is metastable with respect to state 'b', and *vice versa* for $Z_f^* - Z_b^* < 0$. This is the plan for the remainder of the present section.

Calculating the variations for states 'f' and 'b', one finally obtains

$$\delta Z_f^* = (p_0^* - p_v^*)\,\delta V_v^* + (p_0^* - p_l^* - \Pi^*)\,\delta V_l^* + (\mu_l^* - \mu_{sl}^*)\,\delta n_l^* + (\mu_v^* - \mu_{sl}^*)\,\delta n_v^*$$

$$\delta Z_b^* = (p_0^* - p_v^*)\,\delta V_v^* + (\mu_v^* - \mu_{sv}^*)\,\delta n_v^*$$

Here it has been taken into account that $\delta T^* = 0$, $\delta p_0^* = 0$, $\delta \mathscr{A}^* = 0$, and besides $\delta n_v^* + \delta n_l^* + \delta n_{sl}^* = 0$, $\delta V_l^* = \mathscr{A}^*\,\delta\xi^*$ for state 'f', and $\delta n_v^* + \delta n_{sv}^* = 0$ for state 'b'. Use has also been made

of the Gibbs-Duhem relations $-V_l^*\,\delta p_l^* + n_l^*\,\delta\mu_l^* = 0$, $-V_v^*\,\delta p_v^* + n_v^*\,\delta\mu_v^* = 0$ and of the Gibbs adsorption equations $\mathscr{A}^*\,\delta\gamma_{sl}^* + n_{sl}^*\,\delta\mu_{sl}^* = 0$, $\mathscr{A}^*\,\delta\gamma_{sv}^* + n_{sv}^*\,\delta\mu_{sv}^* = 0$, $\delta\gamma^* = 0$,[14] all of them at constant temperature. Note that the quantity

$$\Pi^*(\xi^*) \equiv -d\mathscr{P}^*/d\xi^*$$

appearing in the expression for δZ_f^* has the meaning of the disjoining pressure as one will be able to appreciate by comparing eq 7 with eq 8. As $\mathscr{P}^* \to 0$ as $\xi^* \to +\infty$, one can also write

$$\mathscr{P}^*(\xi^*) = \int_{\xi^*}^{+\infty} \Pi^*(\tilde{\xi}^*)\,d\tilde{\xi}^*$$

Now as δV_v^*, δV_l^*, δn_v^* and δn_l^* for state 'f', and δV_v^* and δn_v^* for state 'b' are independent, the requirements $\delta Z_f^* = 0$, $\delta Z_b^* = 0$ lead to

$$p_v^* = p_0^* \tag{7}$$

for both states,

$$p_l^* = p_0^* - \Pi^*(\xi^*) \tag{8}$$

$$\mu_v^* = \mu_l^* = \mu_{sl}^* \tag{9}$$

for state 'f', and

$$\mu_v^* = \mu_{sv}^* \tag{10}$$

for state 'b'. Note that the values given by eqs 9 and 10 are actually the same since the vapor is at the same pressure and temperature in the two states and hence μ_v^* is the same. Thus, we can write

$$\mu_v^* = \mu_l^* = \mu_{sl}^* = \mu_{sv}^* \equiv \mu^* \tag{11}$$

With eqs 7 and 8, the first equality of eq 11, the fact that the function $\mu_l^* = \mu_l^*(p_l^*, T^*)$ has the

classical form within the ansatz of eq 4, and on account of the definition of Δp^* (cf. the paragraph preceding eq 1), we see that eq 2, introduced earlier in a more naive way, is recovered here. Below, we shall use $\xi^* = \xi_f^*$ as far as state 'f' is concerned. Thus, we finally obtain

$$Z_f^* = \left(\gamma_{sl}^* + \gamma^* + \mathscr{P}^*(\xi_f^*) + \xi_f^* \Pi^*(\xi_f^*)\right) \mathscr{A}^* + \mu^* n^*$$

$$Z_b^* = \gamma_{sv}^* \mathscr{A}^* + \mu^* n^*$$

and

$$(Z_f^* - Z_b^*)/\mathscr{A}^* = \mathscr{P}^*(\xi_f^*) + \xi_f^* \Pi^*(\xi_f^*) - S^* \tag{12}$$

where

$$S^* \equiv \gamma_{sv}^* - (\gamma_{sl}^* + \gamma^*) \tag{13}$$

is the spreading coefficient. Note here that in the framework of the present approach, S^* is an entity generally independent of $\mathscr{P}^* = \mathscr{P}^*(\xi^*)$ and of $\mathscr{P}^*(0)$ in particular (cf. the fourth paragraph of Appendix A).

Now the sought criterion is expressed in terms of the sign of the right-hand side of eq 12. We see that the microfilm $\xi^* = \xi_f^*$ is stable with respect to a bare surface if $S^* > \mathscr{P}^*(\xi_f^*) + \xi_f^* \Pi^*(\xi_f^*)$ and metastable otherwise (i.e. if $S^* < \mathscr{P}^*(\xi_f^*) + \Pi^*(\xi_f^*)\,\xi_f^*$), the marginal condition being just $S^* = \mathscr{P}^*(\xi_f^*) + \xi_f^* \Pi^*(\xi_f^*)$, where recall that ξ_f^* is determined from $\Pi^*(\xi_f^*) = \Delta p^* \propto \Delta T^*$. This amounts to having, for a given $\mathscr{P}^*(\xi^*)$, a critical value of the spreading coefficient, $S_{cr}^* = \mathscr{P}^*(\xi_f^*) + \xi_f^* \Pi^*(\xi_f^*)$, which is a function of the parameters of the system, ΔT^* among them (entering in the above formula through ξ_f^*). Note that $S_{cr}^* > 0$ ($\mathscr{P}^*$ and Π^* being positive decreasing functions of ξ^*), so that we are, interestingly, still within the case of perfect wetting at $S^* = S_{cr}^*$ (i.e. at the moment the extended microfilm turns metastable with respect to a bare surface). Physically, however, as ΔT^* is a possible control parameter while S^* is a material property among many others, a representation of the marginal condition in terms of a critical superheat, $\Delta T^* = \Delta T_{cr}^*$, may be more suitable, where ΔT_{cr}^* is a function of the parameters of the system, S^* among them.

Yet a discussion in terms of S^*_{cr} will be more convenient in the framework of the present paper. On the other hand, as anticipated in section I, for given $S^* > 0$ and $\mathscr{P}^*(\xi^*)$, the occurrence of the metastability of the microfilm can be seen to coincide with its thickness getting smaller than the one of the "pancake".[2,9–11] Recall that the latter is a thin puddle of macroscopic volume of a perfectly-wetting non-volatile liquid that can no longer spread on the solid surface, and whose thickness, say ξ^*_p, is well determined and given by the equation $S^* = \mathscr{P}^*(\xi^*_p) + \xi^*_p \Pi^*(\xi^*_p)$. In the case $\Pi^*(\xi^*) = A^*/\xi^{*3}$ (i.e. $\mathscr{P}^*(\xi^*) = A^*/2\xi^{*2}$) with $A^* > 0$ we shall follow for the most part of the paper, assuming where appropriate the linearization that led to eq 1, the concrete expressions, in supplement to eq 3, for the quantities mentioned above are

$$\xi^*_p = \left(\frac{3\gamma^*}{2S^*}\right)^{1/2} a^*, \quad S^*_{\rm cr} = \frac{3a^{*2}}{2\xi^{*2}_f}\gamma^*, \quad \Delta T^*_{cr} = \frac{T^*_0}{\mathscr{L}^*\rho^*_l A^{*1/2}}\left(\frac{2S^*}{3}\right)^{3/2} \tag{14}$$

where

$$a^* = (A^*/\gamma^*)^{1/2} \tag{15}$$

is a molecular length scale often introduced by de Gennes and coworkers.[2,9–11] As soon as the extended microfilm turns metastable with respect to a bare surface (the criterion for which has been expressed here in three different, albeit of course equivalent, ways: $S^* < S^*_{cr}$, equivalently to $\Delta T^* > \Delta T^*_{cr}$, or to $\xi^*_f < \xi^*_p$), we expect that it is a truncated microfilm that will be present at the contact line, which will no longer extend to cover the adjacent dry spots of the solid surface. The corresponding solutions of the film equation describing the microstructure of the contact line are considered in the following sections. Note also that a few examples concerning the mutual stability of the microfilm and the bare surface beyond the paradigm $\{S^*, \mathscr{P}^*(\xi^*) = A^*/2\xi^{*2}\}$ used here are considered in Appendix A, all involving simple forms of $\mathscr{P}^*(\xi^*)$ and $\Pi^*(\xi^*)$ bounded as $\xi^* \to 0$, albeit still with a positive decreasing asymptotics at larger ξ^*.

IV. Evolution Equation for the Film Thickness

Hereafter, we shall use the notation

$$f^* = [f]\, f \tag{16}$$

where f (without asterisk) is the dimensionless version of a dimensional quantity f^* (with asterisk), $[f]$ being the scale. As already mentioned in section II, attention is limited to the planar geometry. We aim to describe the film structure and dynamics on the scale of the microfilm (eq 3) or, more generally, within the configuration presented in section II and Figure 1, and at the same time intend to carry it out in the framework of the lubrication approximation. Accordingly, we choose the following scales: $[\xi] = [z] = \xi_f^*$, $[x] = \xi_f^{*2}/\sqrt{3}a^*$ (on which the Laplace and disjoining pressures are of the same order, and where $\varepsilon \equiv [\xi]/[x]$ is assumed to be small), $[t] = 3\,\eta_l^*\,\xi_f^*/\gamma^*\varepsilon^4$, and $[\Pi^*] = \Delta p^*$. Then the lubrication equation governing the film evolution $\xi = \xi(x,t)$ can be written as[7]

$$\frac{\partial \xi}{\partial t} + \frac{1}{3}\frac{\partial}{\partial x}\left[\xi^3 \frac{\partial}{\partial x}\left(3\frac{\partial^2 \xi}{\partial x^2} + \Pi(\xi)\right)\right] + E\, j = 0 \tag{17}$$

with

$$j = \frac{1 - \Pi(\xi) - 3\,\partial^2\xi/\partial x^2}{\xi + K}, \qquad \Pi(\xi) = \frac{1}{\xi^3} \tag{18}$$

The dimensionless numbers are

$$\varepsilon = \frac{\sqrt{3}a^*}{\xi_f^*}, \quad E = \frac{\eta_l^*\,\lambda_l^*\,T_0^*}{3a^{*2}\,(\mathscr{L}^*\,\rho_l^*)^2}, \quad K = \frac{2-\phi}{\phi}\sqrt{\frac{\pi R_g^* T_0^*}{2M_w^*}}\,\frac{\lambda_l^*\,T_0^*}{\rho_v^*\,\mathscr{L}^{*2}\,\xi_f^*} \tag{19}$$

where note that ε is not explicitly involved in eq 17 with eq 18. For the notations not yet explained, η^* is the dynamic viscosity, λ^* is the thermal conductivity, R_g^* is the gas constant, M_w^* is the molecular weight, and ϕ is an accommodation coefficient in the evaporation kinetics (a macroscopic phenomenological parameter, not specific to thin films in this model). The quantity j in eq 18 represents the local evaporation flux, with the scales $[j] = \lambda_l^*\,\Delta T^*/\mathscr{L}^*\xi_f^*$ for the mass flux and $[j] = \lambda_l^*\,\Delta T^*/\xi_f^*$ for the associated heat flux. The numerator different from unity is due to the (earlier mentioned) Kelvin effects owing to the disjoining and Laplace pressures, locally

shifting the saturation temperature for a given vapor pressure. In the denominator, the term with K, referred to as the kinetic resistance number, is a consequence of accounting for a finite-rate evaporation kinetics. In the limit $K = 0$, local phase equilibrium prevails at the interface, whereas the evaporation flux is determined by heat conduction from the substrate through the liquid film ("conduction-limited" regime). In the opposite case, $K \gg 1$, the interface temperature is equal to that of the solid support and the flux is determined exclusively by the evaporation kinetics ("kinetics-limited" regime). E is called the evaporation number and quantifies the role of evaporation on the film dynamics on the microscales adjusted such that the disjoining and Laplace pressure effects are formally both of order unity. $E \ll 1$ corresponds to the limit of weak evaporation on these microscales, whereas for $E \gg 1$ the effect of evaporation is expected to be strong. For large values of K, it is rather E/K that plays the role of the evaporation number in this sense. Generally, we imply $E = O(1)$ and $K = O(1)$. Yet one formally needs

$$\varepsilon \ll 1$$

both for the lubrication approximation to hold ($[\xi] \ll [x]$) and for the macroscopic approach to be valid ($a^* \ll \xi_f^*$). For the parameters of Stephan and Busse[5] (ammonia on aluminum at 300 K, see also elsewhere[7]), we have $\varepsilon = 0.58$, $E = 0.124$ and $K = 5.74$. The second example of Morris[6] corresponds to $\varepsilon = 0.45$, $E = 7$ and $K = 50$. Up to notations and scaling factors, and excluding additional physical effects sometimes incorporated into the model, eq 17 with eq 18 is of course the same as elsewhere,[5,6,8] while for a more detailed presentation in the same terms as here see an earlier work of the present authors.[7] However, it is worthwhile emphasizing the key features of the classical model used here such as its one-sidedness (in particular, the vapor pressure inhomogeneity is considered to be negligible,[15] and so is heat conduction into the vapor) and the constancy of the wall temperature (on the scales considered here).

V. Steady Microstructure: Truncated-Microfilm Solutions

Now, in order to solve for the *steady* microstructure of the contact line (Figure 1), either when the contact line remains at rest (steady meniscus) or when its displacement velocity is much smaller than the corresponding microscale $[x]/[t] = \gamma^* \varepsilon^3 / 3\eta_l^*$ (which actually tends to be rather large in practice[7]), one uses a steady version of eqs 17 and 18:

$$\frac{1}{3}\frac{d}{dx}\left[\xi^3 \frac{d}{dx}\left(3\frac{d^2\xi}{dx^2} + \frac{1}{\xi^3}\right)\right] + E\frac{1 - 1/\xi^3 - 3\,d^2\xi/dx^2}{\xi + K} = 0 \tag{20}$$

with the boundary condition

$$\xi \sim b\,x \quad \text{as } x \to +\infty \tag{21}$$

reflecting the assumption that the macroscopic curvature is negligible on the microscales characterizing the microstructure, which in the steady case corresponds to a constant slope at infinity. In the case of an extended microfilm (i.e. a semi-infinite one of constant thickness), the boundary condition at the opposite end is

$$\xi = 1 \quad \text{as } x \to -\infty \tag{22}$$

The coefficient $b = b(E,K)$ is a nonlinear *eigenvalue* of the boundary-value problem represented by eqs 20-22, an extensive parametric study of which is presented elsewhere.[7] Once b is calculated, the apparent contact angle yielded by the microstructure is given by

$$\theta = \varepsilon\, b \tag{23}$$

Thus, in the physical context considered here, it turns out that the microstructure is independent (to leading order) from what happens on larger scales, and moreover imposes the constraint given by eq 23 on this larger-scale behavior.

For what follows, it is worth mentioning that an asymptotic solution of eq 20 satisfying eq 22

can be represented near $\xi = 1$ in the form

$$\xi = 1 + C_1 \exp x + C_2 \exp\left(\sqrt{\frac{3E}{1+K}}x\right) + \ldots \quad \text{as } x \to -\infty \tag{24}$$

(certain further intricacies are discussed elsewhere[7]) with two arbitrary coefficients C_1 and C_2. In the framework of the boundary-value problem given by eqs 20-22, one of them, say C_1, can still be chosen arbitrarily (except for the sign): it just fixes the reference along x without otherwise changing the solution. But then the other must take quite a definite value $C_2 = C_2(E,K)$ in order to be compatible with the behavior given by eq 21.

In the case of a truncated microfilm we are interested in here, instead of eq 22, we look for a solution starting like

$$\xi \sim (4/3)^{1/4}(x - x_0)^{1/2} \quad \text{as } x \to x_0 \tag{25}$$

Now the boundary-value problem is given by eqs 20, 21 and 25, and posed in the interval $x_0 < x < +\infty$.

Such a form of an abrupt film start can often be encountered in the studies of de Gennes and collaborators.[2,9–11,16] It is compatible with our eq 20. Mathematically, this concrete power law is a consequence of the assumption that the disjoining pressure isotherm in the form $\Pi^*(\xi^*) = A^*/\xi^{*3}$ ($A^* > 0$) extends well into the range of thicknesses smaller than the significant thickness scale of the problem (i.e. ξ_f^* as of here), formally up to $\xi^* = 0$. Needless to say that, physically, the behavior given by eq 25 cannot be valid in a sufficiently small region near $x = x_0$, the resolution of which however is not needed within (and remains beyond the scope of) the model under consideration. From such a viewpoint, the behavior given by eq 25 represents just an intermediate asymptotics between this disregarded small initial region on the one hand and the microstructure region figuring in the present study on the other hand (cf. also the second paragraph of Appendix A).

Just as with eq 24 in the case of eq 22, it is worth developing a more detailed asymptotic representation behind eq 25. Pursuing to higher-order terms, it turns out that a solution of eq 20 satisfying eq 25 behaves as (assuming that $K \neq 0$)

$$\xi = \left(\frac{4}{3}\right)^{1/4} (x-x_0)^{1/2} \left[1 + q_1 (x-x_0) + \frac{2^{3/2}}{5\times 3^{3/4}}(1+q_2)(x-x_0)^{3/2} + O\left((x-x_0)^2\right)\right] \text{ as } x \to x_0 \tag{26}$$

where q_1 and q_2 are arbitrary coefficients, which determine all higher-order terms. Within the boundary-value problem given by eqs 20, 21 and 25, by analogy with the earlier described extended-microfilm case, q_2 is expected to adopt a particular value: $q_2 = q_2(E,K,q_1)$. Yet q_1 remains free and defines a family of solutions with a truncated microfilm (note that now the reference along x is fixed by x_0, so these must be essentially different solutions). Now we also have $b = b(E,K,q_1)$. Of course, all this does not mean that the solution exists for $-\infty < q_1 < +\infty$: the admissible interval of q_1 remains to be established.

The physical nature of this one-parameter family of solutions is established by relating q_1 with the spreading coefficient S^*. We note that, in accordance with eq 26,

$$\left(\frac{d\xi}{dx}\right)^2 - \frac{1}{3\xi^2} = \frac{4q_1}{\sqrt{3}} \qquad \text{as} \quad x \to x_0 \tag{27}$$

On the other hand, *at thermodynamic equilibrium*, one can derive the following boundary condition at the *micro*-edge of the film:

$$\frac{\gamma^*}{2}\left(\frac{d\xi^*}{dx^*}\right)^2 - \mathscr{P}^*(\xi^*) = -S^* \qquad \text{as} \quad x^* \to x_0^* \tag{28}$$

where in our case $\mathscr{P}^* = A^*/2\xi^{*2}$. A concise derivation of this boundary condition by variation of the free energy is relegated to Appendix B. In principle, as e.g. presented in de Gennes' review,[2] the condition given by eq 28 can also be established by considering two particular equilibrium configurations: Young's contact angle (for $S^* < 0$) and the pancake for ($S^* > 0$), for which the main result (the angle and the thickness, respectively) is known from global thermodynamic considerations; this then allows to fix the integration constant in the first integral of the augmented Young-Laplace equation (see e.g. Appendix B for the latter), in particular leading to the behavior given by 28 in the limit $x^* \to x_0^*$ on account of $\xi^* \to 0$. We now hypothesize that the *micro*-edge

boundary condition remains the same even in an overall non-equilibrium configuration as considered here. If so, establishing the correspondence between the dimensionless and dimensional representations and comparing eq 27 with eq 28, one readily deduces that

$$q_1 = -\frac{1}{2\sqrt{3}}\frac{S^*}{\gamma^*}\frac{\xi_f^{*2}}{a^{*2}} = -\frac{\sqrt{3}}{4}\frac{S^*}{S_{cr}^*} \tag{29}$$

where the second equality is written on account of eq 14. A further *a posteriori* justification of eq 29 is that the results hereby obtained from eq 20 prove to be compatible with the general (essentially thermodynamic) argument laid out in section III, as will be appreciated in the following two sections.

VI. Parametric Study of the Steady Microstructure

Here we study the steady microstructure of the contact line with a truncated microfilm. The corresponding boundary-value problem represented by eqs 20, 21 and 25 is solved numerically by means of the shooting method. The shooting proceeds from eq 26 approximated at some $x = x_0 + \delta$ ($\delta > 0$ being a small value). For any given q_1, one adjusts the value of q_2 as to observe the behavior specified by eq 21. Hence $q_2 = q_2(E, K, q_1)$, as mentioned earlier.

In doing so, just one solution is found to exist for $q_1 > -\sqrt{3}/4$, and no solution for $q_1 < -\sqrt{3}/4$. Of course, given the numerical character of the calculation, one cannot obtain the critical value for such a transition at exactly $q_1 = -\sqrt{3}/4$. One can only claim that the transition takes place sufficiently close to this value (for instance, a numerical solution can be found for $q_1 = -0.4430$, whereas for $q_1 = -0.4431$ already not). However, there is an argument based on eqs 20 and 26 in favor of placing the transition nonetheless at exactly $q_1 = -\sqrt{3}/4$ (even though this cannot be considered as a rigorous proof either). Indeed, it has been numerically observed that, as q_1 approaches the transition value (from the right side), the truncated microfilm elongates more and more, so that it seems to be perfectly reasonable to conjecture that it turns into the extended one at the transition value (some illustrations are provided below). But when becoming infinitely

long, the truncated microfilm must be no different from the earlier mentioned pancake[2,9–11] with the thickness equal to that of the extended microfilm ($\xi = 1$ in dimensionless terms). This pancake is actually described by the equation $3\,d^2\xi/dx^2 + 1/\xi^3 = 1$ and is obviously a solution of eq 20. Integrating once while observing the value $\xi = 1$ at infinity yields $3\,(d\xi/dx)^2 = 1/\xi^2 + 2\xi - 3$. Using eq 26 in here, one obtains $q_2 = 0$ and $q_1 = -\sqrt{3}/4$ (exactly), which finalizes the argument in question.

In view of eq 29, this critical value $q_1 = -\sqrt{3}/4$ corresponds in fact to $S^* = S^*_{cr}$. Thus, the microstructure with a truncated microfilm exists just for $S^* < S^*_{cr}$. As for the one with a semi-infinite microfilm of constant thickness, the corresponding solution formally exists irrespective of the value of S^* (and does not depend on S^*), for the simple reason that the solid-liquid and liquid-vapor interfaces remain well apart in this configuration and S^* does not appear in the boundary-value problem given by eqs 20-22.

Based on the arguments of section III, of the two microstructure regimes coexisting for $S^* < S^*_{cr}$, the one with a truncated microfilm should be preferred, even though both are deemed to be linearly stable. The extended-microfilm regime should be preferred for $S^* > S^*_{cr}$, but here such a preference is trivial as no truncated-microfilm regime exists in this case. Another argument in favor of this scenario can be found in the following section, where it is seen that the microfilm fronts recede for $S^* < S^*_{cr}$ and advance for $S^* > S^*_{cr}$.

The microstructure profiles with truncated microfilms are shown in Figure 2 for a number of S^*/S^*_{cr} values. The reference along x is set such that $x_0 = 0$. The E and K values are taken based on the Stephan and Busse example[5] (cf. section IV). As S^*/S^*_{cr} approaches unity, the microfilm tail is seen to elongate (as it has already been mentioned above in relation with q_1). It is deemed to become infinitely long in the limit $S^*/S^*_{cr} \to 1$, and thus the profile with a semi-infinite microfilm of constant thickness is in fact a limiting case within the family of truncated profiles. We observe that the tail length is extremely sensitive to the value of S^*/S^*_{cr} when the latter is close to unity. On the other hand, for small enough positive S^*/S^*_{cr} (not to mention the negative S^*/S^*_{cr} – the case of partial wetting), the microfilm tail practically vanishes, even though we still formally refer to the

microstructure as being with a "truncated microfilm".

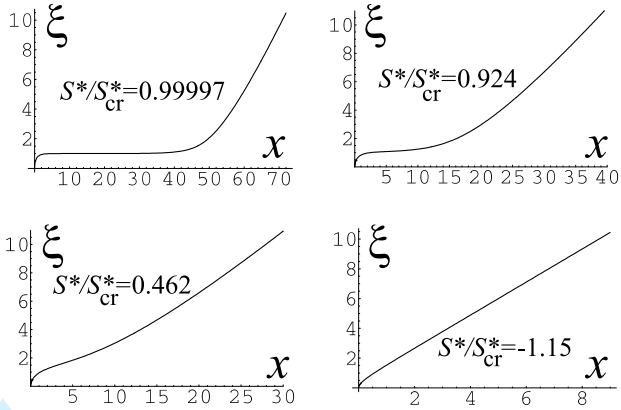

Figure 2: Liquid film profiles for $E = 0.124$, $K = 5.74$ and various values of the spreading coefficient.

The rescaled final slope b is $b = b(E, K, q_1)$ for the regime with a truncated microfilm. Or, on account of eq 29, we have the functional dependence $b = b(E, K, S^*/S^*_{cr})$. Shown in Figure 3 is b versus S^*/S^*_{cr} for a number of pairs of values of E and K, the first two of which are the ones mentioned in section IV and Figure 2, while the other two just serve to appreciate the effect of varying E and K. Also shown are the slopes $b = b(E, K)$, independent of S^*, for the regime with a semi-infinite microfilm of constant thickness. We observe that in the case of perfect wetting ($S^* > 0$) the difference in b between the two regimes is rather insignificant, just up to a few percent. It is only in the partial wetting case ($S^* < 0$) that the difference becomes substantial as the result for the truncated-microfilm regime asymptotically approaches Young's law

$$b = \sqrt{-S^*/S^*_{cr}} \tag{30}$$

as $|S^*|$ is increased. Indeed, in terms of θ and in the framework of the thin-film (lubrication) approximation used here throughout, Young's law has the form

$$\theta = \sqrt{-2S^*/\gamma^*}$$

which can be rewritten as eq 30 in terms of b on account of eqs 14, 19 and 23. In equilibrium

(be it with volatile or non-volatile liquids), Young's law is observed for $S^* < 0$ starting straight from $S^* = 0$, of course, whereas in the present non-equilibrium setup (with a non-zero superheat), it is attained just in the limit of large enough $|S^*|$. On the one hand, this clearly shows that the contact angle becomes just weakly affected by evaporation when the Young's angle is large enough (at fixed superheat). On the other hand, for any given S^*, the "equilibrium limit" (i.e. Young's law represented by eq 30 for $S^* < 0$, and $b = 0$ for $S^* \geq 0$) is also formally approached as the evaporation number E is decreased (the limit of weak evaporation, cf. section IV), even though this does not imply vanishing superheats or thus a true equilibrium, for E does not depend on ΔT^* as one can see in eq 19. This tendency can be appreciated from case IV of Figure 3.

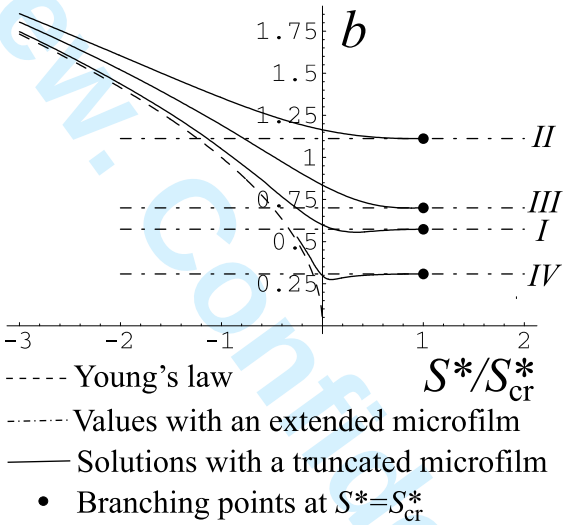

Figure 3: Rescaled apparent contact angle b versus the spreading coefficient. Cases shown: (I) $E = 0.124$, $K = 5.74$; (II) $E = 7$, $K = 50$; (III) $E = 0.124$, $K = 1/10$; (IV) $E = 0.01$, $K = 5.74$. The true apparent contact angle resulting from the microstructure is then $\theta = \varepsilon\, b$, cf. eq 23, with relevant definitions given in eqs 3, 14, 15 and 19.

Finally, it is also of interest to show how the distribution along the film of the local flux, eq 18, looks like in the truncated-microfilm regime, which is done in Figure 4. The fourth curve (to the right) is virtually indistinguishable from that in the extended-microfilm regime. Otherwise, it is important to notice that j remains finite as $x \to x_0$ ($x_0 = 0$ in the figure), as one can in particular establish from eqs 18 and 26. It is also possible to check that neither the pressure in the liquid nor the viscous stress diverge for $x \to x_0$.

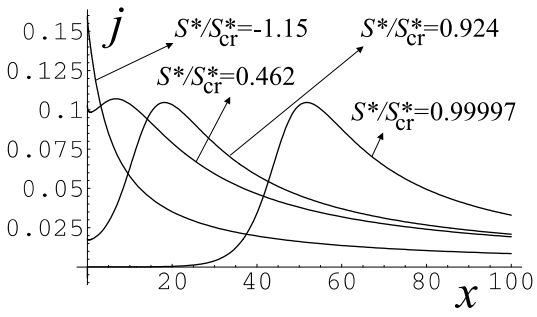

Figure 4: Distributions of the local evaporation flux. The same cases as in Figure 2 are shown.

VII. Traveling Microfilm Fronts

As a complement to the analysis and, more specifically, as an additional illustration to the regime preference discussed above, here we consider propagation of the fronts formed by the extended microfilm. We look for a solution of eq 17 with eq 18 in the form of a traveling wave $\xi = \xi(\tilde{x})$, $\tilde{x} = x + ct$. The equation becomes

$$c\frac{d\xi}{d\tilde{x}} + \frac{1}{3}\frac{d}{d\tilde{x}}\left[\xi^3\frac{d}{d\tilde{x}}\left(3\frac{d^2\xi}{d\tilde{x}^2} + \frac{1}{\xi^3}\right)\right] + E\frac{1 - 1/\xi^3 - 3d^2\xi/d\tilde{x}^2}{\xi + K} = 0 \tag{31}$$

The boundary conditions specific to such a microfilm front are (cf. eqs 22 and 25)

$$\xi \sim (4/3)^{1/4}\tilde{x}^{1/2} \quad \text{as } \tilde{x} \to 0, \qquad \xi = 1 \quad \text{as } \tilde{x} \to +\infty \tag{32}$$

The front velocity c is an eigenvalue of the boundary-value problem given by eqs 31 and 32. An advancing front would correspond to $c > 0$, while a receding one to $c < 0$.

The counterpart of the asymptotic expansion represented by eq 26 is now

$$\xi = \left(\frac{4}{3}\right)^{1/4}\tilde{x}^{1/2}\left[1 + q_1\tilde{x} - \frac{2^{1/2}3^{3/4}}{5}c\tilde{x}^{3/2}\log\tilde{x} + \frac{2^{3/2}}{5\times 3^{3/4}}(1+q_2)\tilde{x}^{3/2} + O\left(\tilde{x}^2\log\tilde{x}\right)\right] \text{ as } \tilde{x} \to 0 \tag{33}$$

where q_1 is related to the spreading coefficient by means of eq 29, i.e. equilibrium is still assumed at the micro-edge. Let us underscore that, importantly, no critical (non-integrable) divergences are associated with the behavior given by eq 33 (which is in fact singular in itself, cf. a brief discussion

following eq 25), even in the present case of a moving truncated-microfilm edge ($c \neq 0$). Indeed, one can show using the lubrication theory that, with eq 33, the dissipation density in the film (per unit area of the solid surface) behaves as $\sim c^2/\sqrt{\tilde{x}}$ as $\tilde{x} \to 0$, which, even though diverging, is integrable. The same can be said about the tangential stress exerted on the substrate, behaving as $\sim c/\sqrt{\tilde{x}}$ as $\tilde{x} \to 0$, and about the local evaporation flux (eq 18), whose divergence is even weaker, viz. $j \sim c \log\tilde{x}$ as $\tilde{x} \to 0$.

The problem is again solved using the shooting method. Now two parameters — c and q_2 — need to be adjusted in order to ensure the required behavior as $\tilde{x} \to +\infty$. Thus, we obtain $c = c(E, K, S^*/S^*_{cr})$, $q_2 = q_2(E, K, S^*/S^*_{cr})$. Note that for $S^* = S^*_{cr}$ (i.e. $q_1 = -\sqrt{3}/4$), the solution is with $c = 0$ and $q_2 = 0$ and satisfies the equation $1/\xi^3 + 3\,d^2\xi/d\tilde{x}^2 = 1$. In fact, this motionless front is again the pancake solution[2,9–11] (implying that, ideally, the pancake is infinitely long and that the front in question describes one of its edges), as already discussed in the beginning of section VI.

The resulting dependence of c on S^*/S^*_{cr} is shown in Figure 5 for the same cases as in Figure 3. We see that the fronts are advancing for $S^* > S^*_{cr}$ (the microfilm spreads to cover all the surface of the substrate) and receding for $S^* < S^*_{cr}$. Thus, we appreciate that the ansatz given by eq 29 has led us to reasonable results in this and the previous sections, coherently with the considerations made in section III on thermodynamic grounds. Let us also mention the dimensional scale $[c] = [x]/[t] = \gamma^* \varepsilon^3/3\eta_l^*$ (cf. the notation given by eq 16), which can be rather large, as already pointed out in the beginning of section V.

Some front profiles are shown in Figure 6. A noteworthy feature is a ridge present in the receding front, which points to the possibility of developing a fingering instability, as one would expect based upon the study by Lyushnin et al.[17] Note though that the mentioned study considers, speaking in our terms, a front (kink) between two different extended-microfilm states, which can exist for an appropriate form of the disjoining pressure tail (e.g. involving positive local maximum and minimum, as it can be the case for polar liquids), whereas here we consider a front between the (only possible) microfilm and a bare surface for a simpler disjoining pressure tail, in the form

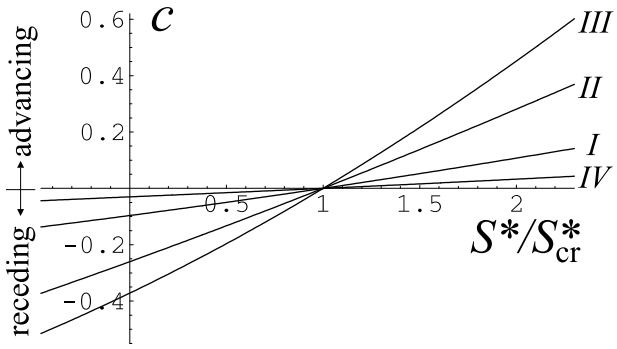

Figure 5: The velocity of the microfilm front versus the spreading coefficient. Cases shown are those of Figure 3.

of a positive inverse cubic law typical for non-polar liquids. Another noteworthy feature here is that, for sufficiently large velocity (sufficiently large values of $(1 - S^*/S^*_{cr})$), a receding front can become wavy, meaning that the state $\xi = 1$ is attained in an oscillatory fashion as $\tilde{x} \to +\infty$. To establish when this happens, it is just sufficient to linearize eq 31 near $\xi = 1$ and calculate the eigenvalues.[7]

Finally, it is interesting to note that the behavior given by eq 33 is valid not only in a volatile-liquid case as considered here, but also in the case of a non-volatile liquid, recovered non-singularly within eq 33 by letting $E = 0$ (in fact, not enough terms are written down in the series of eq 33 to appreciate the difference between $E \neq 0$ and $E = 0$). In this connection, as far as the non-volatile case is concerned, let us point out that the family of solutions with truncated precursor films for a moving contact line obtained by Hervet and de Gennes[16] must satisfy eq 33 (with $E = 0$ and rescaled to their notations). Therefore, when being calculated by means of a shooting procedure, these solutions could well be started from eq 33, where q_1 still gets related to the spreading coefficient through eq 28 (but the concrete expression will be different from eq 29 in their notations, of course), while q_2 is adjusted in order to have $d^2\xi/d\tilde{x}^2 = 0$ as $\tilde{x} \to +\infty$. In Hervet and de Gennes,[16] however, a different way of shooting was used. Namely, they shot from a large value of $\tilde{x}$, where $d^2\xi/d\tilde{x}^2 = 0$ was deemed to hold with a sufficient precision, towards smaller values of $\tilde{x}$, eventually recovering the behavior of eq 25 (where the tilde should be placed over the x symbols in the notations of the present section). By varying the slope $d\xi/d\tilde{x}$ at the starting point

about the corresponding slope of their "maximal" solution (the latter being formally the one for $S^* = +\infty$), they obtained a one-parameter family of solutions, which could be associated with the spreading coefficient as the parameter of the family by means of eq 28 rewritten in the appropriate dimensionless form.

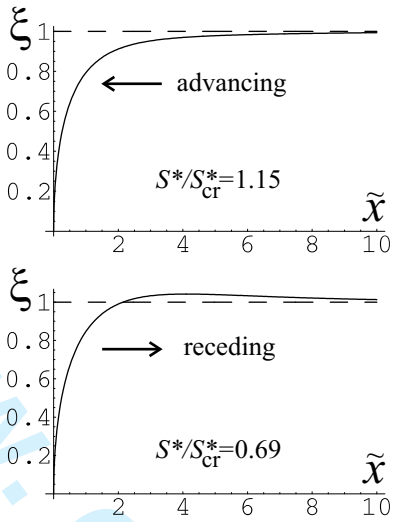

Figure 6: Examples of the microfilm front profiles: a receding front (with a ridge) for $S^* < S^*_{cr}$ and an advancing one for $S^* > S^*_{cr}$ ($E = 0.124$, $K = 5.74$).

VIII. Conclusions

The present paper has been centered upon the investigation, as a function of the spreading coefficient S^*, of the steady microstructure of a pure-vapor/liquid contact line on a superheated substrate, the disjoining pressure being a positive inverse cubic law in particular computations. We have adhered to an approach based upon a separation of scales in the sense that the disjoining pressure is applied at the thicknesses for which the continuum physics is deemed to be still valid, whereas otherwise the state of the vapor-solid interface is described by an appropriate surface tension (entering the definition of the spreading coefficient) following the Gibbs adsorption theory. In the framework of such an approach, S^* is an independent (from the disjoining pressure isotherm) parameter of the problem.

For the stated form of the disjoining pressure, there always exists a classical microstructure

regime, independent of S^*, with an extended microfilm (whose thickness decreases with the superheat $\Delta T^* > 0$) covering all the adjacent "dry" parts of the solid surface. We have argued, however, on both thermodynamic and film-dynamics grounds that this extended-microfilm regime becomes metastable with respect to a new, truncated-microfilm regime when the spreading coefficient happens to be below a critical value S^*_{cr}, the latter being (remarkably) positive (and increasing with the superheat). Turning the view around in the parameter space, instead of S^*_{cr}, one can speak of a critical superheat at a given S^*. While for $S^* < 0$ it is always the truncated-microfilm regime that is preferred (is more stable), for a given $S^* > 0$ there exists a critical value ΔT^*_{cr} of ΔT^*, below which we expect the extended-microfilm regime, and above which the truncated-microfilm regime should be chosen. Quite remarkably, passing over the critical condition corresponds to the extended-microfilm thickness (a decreasing function of ΔT^*) falling below the thickness of the pancake (a decreasing function of $S^* > 0$) considered by de Gennes and coworkers.

More specifically, the thermodynamic argument has been developed by analyzing the mutual stability of the microfilm and "bare"-surface states. Under the conditions when the former is metastable with respect to the latter, it can be conjectured that the contact line microstructure must be with a truncated microfilm rather than with an extended one, and vice versa. Thus, the results formulated in the previous paragraph have first been conjectured already on the basis of thermodynamic considerations alone. Importantly though, they have subsequently proved to be fully coherent with simulations based upon a classical lubrication film equation (one-sided model) with a (positive) inverse cubic law for the disjoining pressure and the equilibrium condition assumed at the front edge (should there be one) where the film thickness vanishes, the simulations besides providing some additional details. The truncated-microfilm regime has thereby been found just for $S^* < S^*_{cr}$ (i.e. $\Delta T^* > \Delta T^*_{cr}$), where it should be preferred over the extended-microfilm one according to the thermodynamic argument. The latter regime should be preferred for $S^* > S^*_{cr}$ (i.e. $0 < \Delta T^* < \Delta T^*_{cr}$), all the more so as it remains the only one in this region of the parameter space according to our calculations. Interestingly, there turns out to be a continuous transition between the two regions in the parameter space: as $S^* \to S^*_{cr}$ (from below) or $\Delta T^* \to \Delta T^*_{cr}$ (from above),

the truncated microfilm elongates and eventually extends to infinity. A most clear illustration of the regime preference in the framework of the film evolution equation comes from studying the direction of propagation of traveling microfilm fronts between the extended microfilm and the "bare" surface. It has been confirmed that they are receding under the conditions the truncated-microfilm regime is thermodynamically preferred, and advancing otherwise, which additionally points to the compatibility between the film-dynamics model and the thermodynamic arguments. Notably enough, a receding front is with a ridge, hinting at its possible fingering instability, while an advancing one is not.

The microfilm regime (extended or truncated) has implications on the contact line microstructure as a whole, and most remarkably on the apparent contact angle (an eigenvalue of the steady microstructure problem). Yet, for $S^* > 0$, we have not found any significant difference in the contact angles between the two regimes, just a few percent at most. For $S^* < 0$, however, the difference is more pronounced, the more so, the larger the absolute value of S^* is. In fact, in the latter limit, the evaporation-induced contribution into the contact angle becomes progressively negligible against the value given by Young's law, which is asymptotically attained for the truncated-microfilm regime. In the extended-microfilm regime, however, the contact angle naturally remains the same for all S^* (but this regime is metastable for $S^* < S^*_{cr}$, as said above).

For more general disjoining pressure laws, for which a positive decreasing dependence (e.g. the inverse cubic one) is not imposed elsewhere than asymptotically at large thicknesses, it is clear that the results obtained by formally assuming such a dependence at all thicknesses can be quantitatively valid only for sufficiently small values of S^* and ΔT^*. The qualitative validity may be broader, but even here there may be certain obvious limitations. For instance, while ΔT^*_{cr} may exist for small enough $S^* > 0$, it may disappear for larger $S^* > 0$, which is obviously not the case with a positive inverse cubic law throughout, when ΔT^*_{cr} formally exists at any $S^* > 0$. The examples given in Appendix A for a slightly more general class of disjoining pressures help to see these points more clearly. Nonetheless, the conclusions for these examples are drawn here just based upon the thermodynamic argument. It would be quite of interest, as a future work, to

consider them also in the framework of the film equation and to analyze the resulting form of the truncated-microfilm regime of the contact line microstructure.

Acknowledgement

The authors acknowledge financial support of the European Space Agency and of the Belgian Science Policy through the PRODEX-BOILING project, as well as of the Communauté Française de Belgique through the ARCHIMEDES (ARC 04/09-308) project. The travel support of the Marie Curie ITN Network MULTIFLOW is also greatly appreciated, having allowed quite stimulating discussions with members of the Network. PC also gratefully acknowledges financial support of the Fonds de la Recherche Scientifique - FNRS.

References

(1) Derjaguin, B. V.; Churaev, N. V.; Muller, V. M. *Surface forces*; Consultants Bureau: New York, 1987.

(2) de Gennes, P. G. *Rev. Mod. Phys.* **1985**, *57*, 827–863.

(3) Potash, M.; Wayner, P. C. *Int. J. Heat Mass Transfer* **1972**, *15*, 1851–1863.

(4) Moosman, S.; Homsy, G. M. *J. Colloid Interface Sci.* **1980**, *73*, 212–223.

(5) Stephan, P. C.; Busse, C. A. *Int. J. Heat Mass Transfer* **1992**, *35*, 383–391.

(6) Morris, S. J. S. *J. Fluid Mech.* **2001**, *432*, 1–30.

(7) Rednikov, A. Y.; Rossomme, S.; Colinet, P. *Multiphase Sci. Technol.* **2009**, *21*, 213–248.

(8) Ajaev, V. S. *J. Fluid Mech.* **2005**, *528*, 279–296.

(9) de Gennes, P. G.; Brochard-Wyart, F.; Quéré, D. *Capillarity and wetting phenomena*; Springer, 2004.

(10) Joanny, J. F.; de Gennes, P. G. *C. R. Acad. Sc. Paris* **1984**, *299 II*, 279–283.

(11) Brochard-Wyart, F.; di Meglio, J. M.; Quéré, D.; de Gennes, P. G. *Langmuir* **1991**, *7*, 335–338.

(12) Yeh, E. K.; Newman, J.; Radke, C. J. *Colloids and Surfaces A* **1999**, *156*, 137–144.

(13) Yeh, E. K.; Newman, J.; Radke, C. J. *Colloids and Surfaces A* **1999**, *156*, 525–546.

(14) Defay, R.; Prigogine, I.; Bellemans, A.; Everett, D. H. *Surface tension and adsorption*; Wiley: New York, 1966.

(15) Rednikov, A. Y.; Colinet, P. *Proceedings (CD-ROM) of the EUROTHERM N 84 Seminar on Thermodynamics of Phase Changes*; Namur (Belgium), 2009.

(16) Hervet, H.; de Gennes, P. G. *C. R. Acad. Sc. Paris* **1984**, *299 II*, 499–503.

(17) Lyushnin, A. V.; Golovin, A. A.; Pismen, L. M. *Phys. Rev. E* **2002**, *65*, 021602(7).

Appendix A: Further Outlook and Illustrations

The present appendix touches upon some more in-depth aspects of the analysis. Its main part is dedicated to a few supplementary examples beyond the paradigm $\{S^*, \mathscr{P}^* = A^*/2\xi^{*2}\}$, as foreseen at the end of section III.

The following remark is pertinent as far as the conceptual scheme used in the present paper is concerned. The word 'tail' used with regard to the disjoining pressure isotherm is mostly intended to underscore that it is taken just on the range of film thicknesses where the continuum approach is still valid, and which the extended microfilm clearly belongs to. The concept of the disjoining pressure *is not employed here* below this range (even though it can in principle be extended thereto to formally accommodate for adsorption isotherms and Henry's law in particular, as shown in an example of Yeh et al.[12] and references therein). The "bare-surface" state (characterized by the

appropriate solid-vapor surface tension, entering into the definition of the spreading coefficient) is treated here within the classical thermodynamics of adsorption. The film thickness in this state is formally equal to zero within this scheme, which is justified given its actual smallness on the scale of the continuum range. In fact, this is essentially how we proceed in section III. Thus, it is such a separation of scales in terms of film thicknesses that we conceptually adhere to here. Admittedly, proceeding in this way, there remains a gap where things are not quite well defined. However, this gap is likely to be "integrable through", as we essentially find out here in sections V-VII, where the retribution comes just in the form of a "good" singularity at the edge of the truncated microfilm (cf. the discussion following eq 25). Thus, there is in fact no overwhelming need for being more accurate in this regard, which is not possible at a rigorous level in the framework of the hydrodynamic approach anyway.

For the most part of the present paper, the disjoining pressure (tail) has been assumed to be in the form of an inverse cubic law (typical for non-polar liquids), as in the majority of the studies cited in section I. In a slightly more general class of tails to be evoked in this appendix, the disjoining pressure is still a positive decreasing (fast enough) function at sufficiently large thicknesses, with no such limitation at smaller thicknesses, but with *no minimum* at a finite thickness.

Let us say a few words about the relationship between S^* and $\mathscr{P}^*$. One may adhere to the viewpoint[9] that a continuous transition from a film-covered surface to a bare one implies $S^* = \mathscr{P}^*(0)$. On the other hand, if $\mathscr{P}^* = \mathscr{P}^*(\xi^*)$ represents just the tail of the disjoining pressure isotherm as in the present paper, the entities S^* and $\mathscr{P}^*(\xi^*)$ are essentially independent, so that $S^* \neq \mathscr{P}^*(0)$ does not necessarily contradict the above mentioned viewpoint. Indeed, in this scheme, $\mathscr{P}^*(0)$ is effectively not the "true" value at $\xi^* = 0$ but rather a low-ξ^* limit from the tail. For instance, in the case of a positive inverse cubic law of the disjoining pressure, we have $S^* < \mathscr{P}^*(0)$ for the simple reason that $\mathscr{P}^*(0) \to +\infty$. Interestingly enough, in the case $\mathscr{P}^*(0)$ is finite, a finite equilibrium micro- contact angle can exist on a bare solid surface for $S^* < \mathscr{P}^*(0)$ (the augmented Young relation,[12] see also Appendix B), the angle vanishing for $S^* = \mathscr{P}^*(0)$.

The examples to be considered here are represented in Figure 7(a-d). All of them still observe

the positive inverse cubic law at sufficiently large thicknesses ξ^*, but depart from it at smaller ξ^*. Besides, in the examples chosen here, $\mathscr{P}^*$ and Π^* remain finite as $\xi^* \to 0$. Note also that all of them fall under the more general class of disjoining pressure tails mentioned above. The cases (a) and (b) correspond in fact to figure 4.5 of de Gennes et al.[9] The cases (c) and (d) are similar to (a), but without an inflection point. In (a-c), it is assumed that $S^* = \mathscr{P}^*(0)$, whereas $0 < S^* < \mathscr{P}^*(0)$ in (d) (cf. a brief discussion above). Otherwise, the examples (c) and (d) are identical. In view of eq 2, when working with the disjoining pressure curves as we do in Figure 7, various superheat ΔT^* levels are more conveniently characterized in terms of Δp^*, which is proportional to ΔT^* by means of eq 1.

A necessary (and, in the simple cases under consideration, sufficient) condition for the pancake configuration to exist is that the equation $S^* = \mathscr{P}^*(\xi_p^*) + \xi_p^* \Pi^*(\xi_p^*)$ has a solution ξ_p^*. Graphically, this is equivalent to the existence of a straight tangential line to the curve $\mathscr{P}^* = \mathscr{P}^*(\xi^*)$ emanating from the point $(0, S^*)$ of the $\mathscr{P}^*$ versus ξ^* diagram, the pancake thickness ξ_p^* being given by the abscissa of the point of contact. Thus, the pancake exists in the cases (a) and (d) of Figure 7, where the corresponding tangential lines are drawn, but not in the cases (b) and (c). For comparison, note that in the case of a positive inverse cubic law of the disjoining pressure at all thicknesses ξ^* (i.e. the paradigm $\{S^*, \mathscr{P}^* = A^*/2\xi^{*2}\}$), the pancake always exists for $S^* > 0$ and does not for $S^* < 0$. In the case $S^* = \mathscr{P}^*(0)$, the pancake configuration moreover obeys in the Π^* versus ξ^* diagram the Maxwell rule (of equal areas), as shaded in Figure 7(a). Now, as discussed in the paragraph preceding eq 14, the critical superheat ΔT_{cr}^* (or Δp_{cr}^* in terms of Δp^*, cf. eq 1) is the one corresponding to the pancake, whose level is shown in Figure 7(a,d) by a horizontal line labeled Δp_{cr}^* in the Π^* versus ξ^* diagrams.

We now focus on the case (a) of Figure 7. For a superheat level below critical, as e.g. for the level I, the microfilm is more stable than the bare surface, as the sign of eq 12 is negative, where to understand this negative sign more graphically note that $\mathscr{P}^*(\xi_f^*) + \xi_f^* \Pi^*(\xi_f^*)$ is the intercept on the vertical axis of the tangent to the $\mathscr{P}^*(\xi^*)$ curve at the point $\xi^* = \xi_f^*$ (not shown on the plots). But at the level II the former is rather metastable against the latter. A further superheat increase,

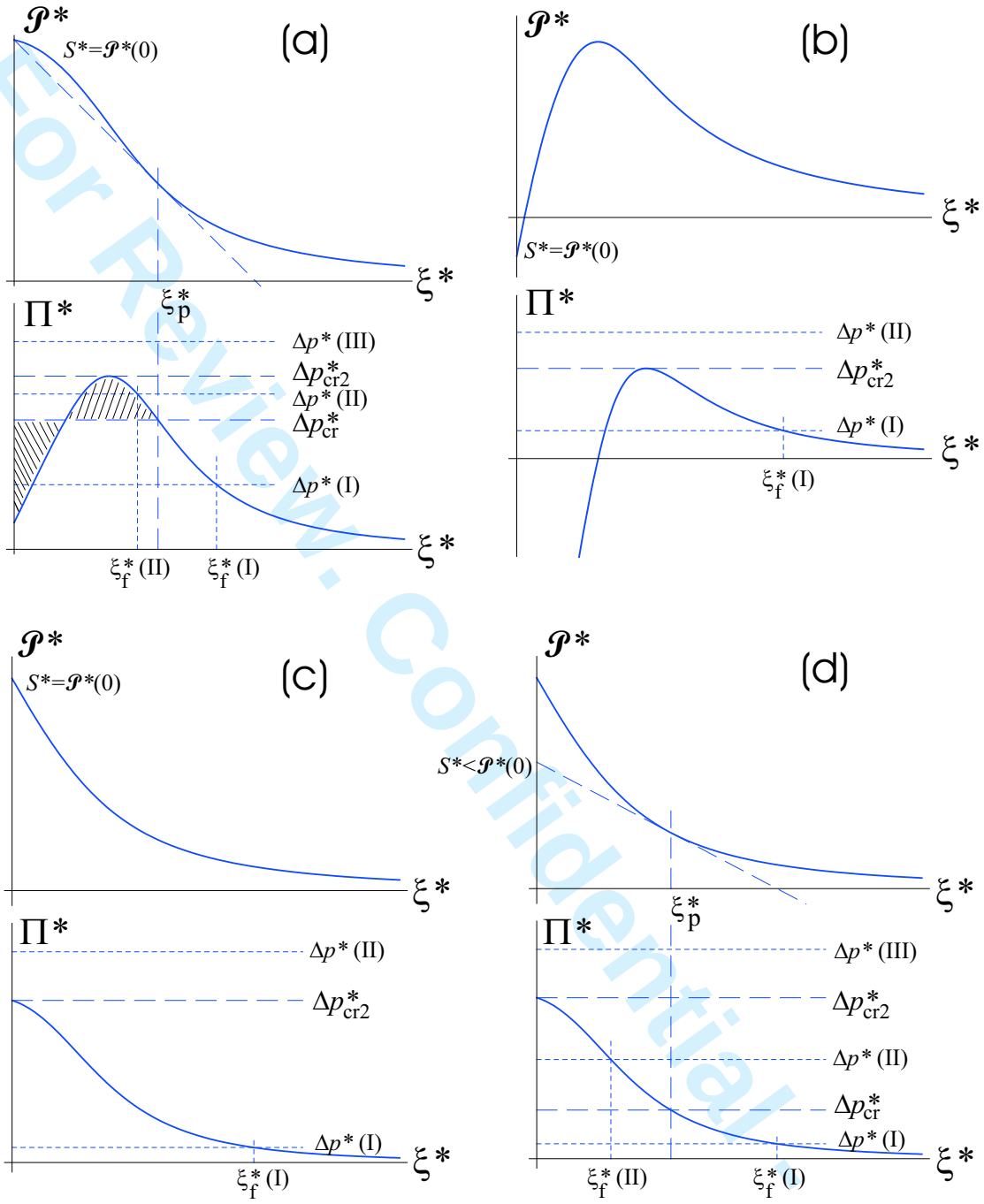

Figure 7: Solid lines: $\mathscr{P}^* = \mathscr{P}^*(\xi^*)$ dependencies together with the associated disjoining pressure isotherms, $\Pi^*(\xi^*) = -d\mathscr{P}^*/d\xi^*$, placed just underneath. Long dashed lines put in evidence the pancake configuration and other critical conditions. Short dashed lines and Roman numerals between the parentheses pertain to the typical superheat levels referred to in the text. Cf. eqs 1 and 2.

above a second critical value ΔT^*_{cr2} (or Δp^*_{cr2}), results in the disappearance of the microfilm state, the bare surface remaining the only possible state, as for the level III. In contrast, note that in the framework of the paradigm $\{S^*, \mathscr{P}^*(\xi^*) = A^*/2\xi^{*2}\}$, the microfilm state always formally exists (even if metastable), so that it is not surprising that no second critical value has arisen earlier in the present paper.

Note that the microfilm state corresponds to solutions of eq 2 at which $d\Pi^*/d\xi^* < 0$. In the examples of Figure 7, there may also be solutions with $d\Pi^*/d\xi^* > 0$, but they must be discarded as (linearly) unstable. While such an instability is a well-known result, it can readily be recovered using the developments of section III. Indeed, with still taking eq 7 and eq 9 (or eq 11) into account but disregarding for the moment eq 8 (or its equivalent eq 2), one obtains the following expression for Z^* at a microfilm state: $Z^* = \left(\gamma^*_{sl} + \gamma^* + \mathscr{P}^*(\xi^*) + \Delta p^*\,\xi^*\right)\mathscr{A}^* + \mu^* n^*$, where Δp^* just stands for $p^*_v - p^*_l$, and is given by eq 1 in view of $\mu^*_v = \mu^*_l$. Now eq 2 (or equivalently eq 8) is recovered from $\partial Z^*/\partial \xi^* = 0$. For the second derivative, one obtains $\partial^2 Z^*/\partial \xi^{*2} = -\mathscr{A}^* d\Pi^*/d\xi^*$, whose negativeness for the states with $d\Pi^*/d\xi^* > 0$ signals to their instability, for the function Z^* then does not present a local minimum.

In the example of Figure 7(b), $S^* < 0$ and, as it has already been pointed out, no pancake exists. So there is no critical superheat value for the change of the thermodynamic stability status of the microfilm state. It is just always metastable, as for instance at the level I. The situation is here not different in this regard from the case of a positive inverse cubic law with $S^* < 0$. However, the difference is that here the metastable microfilm state disappears at all for sufficiently large superheats, rendering the bare-surface state the only one (as at the level II).

On the contrary, in the case (c), where the pancake does not exist either, the microfilm state is stable versus the bare surface until its disappearance, formally at a vanishing thickness, for large enough superheats. The bare-surface state then remains the only one and stable (e.g. as at the level II).

The explanations for the case (d) are mostly the same as those for the case (a). One could notice, however, that even though the microfilm state is metastable with respect to the bare-surface

one at the level II, the domain of attraction (in terms of uniform initial film thicknesses) of the latter state is apparently very small in this case: it must be limited to a narrow zone about $\xi^* = 0$ (beyond the applicability of the continuum approach) where the "singularity" $S^* \neq \mathscr{P}^*(0)$ can be resolved (cf. the discussion earlier in this appendix). In contrast, at the level II of the case (a), the corresponding domain of attraction must extend up to the intermediate, linearly unstable (i.e. $d\Pi^*/d\xi^* > 0$), state.

Thus, we see that, even for a more general class of disjoining pressure tails considered in this appendix, some simple criteria can laid out as far as the existence of the critical superheat ΔT^*_{cr} and the stability status of the extended microfilm versus the bare surface are concerned, for which evoking the pancake configuration of de Gennes and coworkers turns out to be particularly helpful. To recapitulate, one can state the following. If the value of the spreading coefficient and the disjoining pressure function are such that the pancake configuration exists (note for comparison that for a positive inverse cubic law throughout, the pancake formally exists at any $S^* > 0$), then so do ΔT^*_{cr} and the stability status change in question, the critical point corresponding to the moment when, at increasing ΔT^*, the extended-microfilm thickness becomes lower than the pancake thickness. On the other hand, if the pancake does not exist, then there exists no ΔT^*_{cr} either, in the sense that the stability status of the extended-microfilm regime (where the latter exists) should never change as ΔT^* is changed. Thus, for $S^* < 0$ (a priori no pancake in the framework of our assumptions on the form of the disjoining pressure), it should always be metastable versus the bare surface. But should there exist no pancake for $S^* > 0$, actually meaning that this given value of S^* is not sufficiently small (cf. the beginning of this paragraph) for this given disjoining pressure law, the extended-microfilm regime should always be stable where it exists. In this latter case, the paradigm "spreading coefficient + positive inverse cubic law for all thicknesses", used in the most part of the present paper, is not valid even qualitatively as far as the stability status predictions are concerned, since it predicts the existence of ΔT^*_{cr} for any $S^* > 0$. Yet note that this paradigm correctly captures, at least qualitatively, the stability status for $S^* < 0$ on the one hand, and the possible change of the stability status as ΔT^* is increased at $S^* > 0$ under the pancake existence on

the other hand.

Film-dynamics simulations similar to section VI are not carried out for the examples here. Nonetheless, we conjecture (just like in section III, but now perhaps more confidently in view of the results of sections VI and VII) that under the conditions when the microfilm state exists and is stable against the bare surface, it is the extended-microfilm regime of the steady microstructure of a contact line that is preferred. Otherwise, it must be a truncated-microfilm regime.

Appendix B: Equilibrium Condition at the Edge of the Microfilm

Here we derive the equilibrium edge condition given by eq 28. In principle, for this derivation, we could directly refer elsewhere,[12] apart for certain nuances: in particular, unlike the mentioned work,[12] we are generally concerned with a situation where $\mathscr{P}^*$ and $d\xi^*/dx^*$ are formally not assumed to be finite as $x^* \to x_0^*$ (e.g. $\mathscr{P}^* = A^*/2\xi^{*2}$ while $\xi^* \to 0$). We proceed in a planar geometry, and let w^* be the "width" of the system along the third axis (orthogonal to the plane under consideration). Let x_0^* be the coordinate of the edge, the film being located at $x^* > x_0^*$. Let us formally introduce $x_{\min}^*$ and $x_{\max}^*$ ($x_{\min}^* < x_0^* < x_{\max}^*$) limiting the range of x, which will however be rather immaterial in the present consideration, as we are focused on the condition at $x^* = x_0^*$. Then, with eqs 4 and 6, one can write

$$Z^*/w^* = (\mu_l^* n_l^* + \mu_v^* n_v^* + \mu_{sl}^* n_{sl}^* + \mu_{sv}^* n_{sv}^*)/w^* + (p_0^* - p_v^*)V^*/w^* + (p_v^* - p_l^*)\int_{x_0^*}^{x_{\max}^*} \xi^*(\tilde{x}^*)\,d\tilde{x}^*$$

$$+ \gamma_{sv}^*(x_0^* - x_{\min}^*) + (\gamma_{sl}^* + \gamma^*)(x_{\max}^* - x_0^*) + \int_{x_0^*}^{x_{\max}^*} \left[\frac{\gamma^*}{2}\left(\frac{d\xi^*}{dx^*}\right)^2 + \mathscr{P}^*(\xi^*)\right] d\tilde{x}^*$$

where it has been taken into account that

$$d\mathscr{A}_{lv}^* = \sqrt{1 + \left(\frac{d\xi^*}{dx^*}\right)^2}\, w^*\,dx^* \approx \left[1 + \frac{1}{2}\left(\frac{d\xi^*}{dx^*}\right)^2\right] w^*\,dx^*$$

the latter approximation corresponding to the thin-film (lubrication) approximation used throughout the paper. Next, we shall be interested in calculating the variation δZ^* resulting from a displacement δx_0^*. Yet δx_0^* is not independent of $\delta \xi^*$:

$$\delta \xi^* \sim -\frac{d\xi^*}{dx^*}\,\delta x_0^* \qquad \text{as} \quad x^* \to x_0^* \tag{B1}$$

Thus, we calculate δZ^* depending on δx_0^* and $\delta \xi^*$, while the rest of the quantities can be left unvaried for our purposes here (independent variables). We obtain

$$\delta Z^*/w^* = (p_v^* - p_l^*)\int_{x_0^*}^{x_{\max}^*} \delta\xi^*\, d\tilde{x}^* + S^*\,\delta x_0^* - \left[\frac{\gamma^*}{2}\left(\frac{d\xi^*}{dx^*}\right)^2 + \mathscr{P}^*(\xi^*)\right]\Bigg|_{x^*\to x_0^*}\delta x_0^* + \int_{x_0^*}^{x_{\max}^*}\left[\gamma^*\frac{d\xi^*}{dx^*}\frac{d\delta\xi^*}{dx^*} - \Pi^*(\xi^*)\,\delta\xi^*\right] d\tilde{x}^* \tag{B2}$$

where the definition given by eq 13 has been used, and besides, it has been taken into account that $\xi^* \to 0$ as $x^* \to x_0^*$. Integration by parts of the last term in eq B2 yields

$$\gamma^*\frac{d\xi^*}{dx^*}\,\delta\xi^*\Bigg|_{x^*\to x_{\max}^*} - \gamma^*\frac{d\xi^*}{dx^*}\,\delta\xi^*\Bigg|_{x^*\to x_0^*} - \int_{x_0^*}^{x_{\max}^*}\left[\gamma^*\frac{d^2\xi^*}{dx^{*2}} + \Pi^*(\xi^*)\right]\delta\xi^*\, d\tilde{x}^*$$

With this and eq B1, we recover eq 28 from eq B2 as a necessary condition for $\delta Z^* = 0$, while another necessary condition leads to what is referred to as the augmented Young-Laplace equation (here in the thin-film approximation):

$$p_v^* - p_l^* = \gamma^*\frac{d^2\xi^*}{dx^{*2}} + \Pi^*(\xi^*)$$

of which eqs 7 and 8 yield a particular case. It is interesting to note that in the case when $\mathscr{P}^*(0)$ is finite and $S^* \le \mathscr{P}^*(0)$, the condition given by eq 28 corresponds to a *micro-* contact angle at a

bare solid surface

$$\left|\frac{d\xi^*}{dx^*}\right|_{x^*=x_0^*} = \sqrt{2\,\frac{\mathscr{P}^*(0) - S^*}{\gamma^*}}$$

which is called the augmented Young relation [12] (here we have it in the thin-film approximation), the angle becoming equal to zero for $\mathscr{P}^*(0) = S^*$.

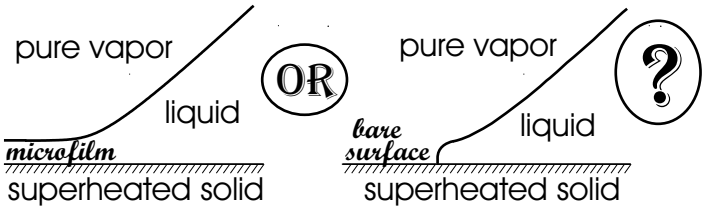

table of contents only